J|A|C|S
ARTICLES
Published on Web 06/08/2002

Pentalenene Synthase. Analysis of Active Site Residues by Site-Directed Mutagenesis

Myriam Seemann,[†] Guangzhi Zhai,[†] Jan-Willem de Kraker,[§] Chiana M. Paschall,[‡] David W. Christianson,[‡] and David E. Cane*,[†]

Contribution from the Department of Chemistry, Box H, Brown University, Providence, Rhode Island 02912-9108, Department of Organic Chemistry, Wageningen Agricultural University, Dreijenplein 8, 6703 HB Wageningen, The Netherlands, Plant Research International, P.O. Box 16, 6700 AA Wageningen, The Netherlands, and Roy and Diana Vagelos Laboratories, Department of Chemistry, University of Pennsylvania, Philadelphia, Pennsylvania 19104-6323

Received February 28, 2002

Abstract: Incubation of farnesyl diphosphate (**1**) with the W308F or W308F/H309F mutants of pentalenene synthase, an enzyme from *Streptomyces* UC5319, yielded pentalenene (**2**), accompanied by varying proportions of (+)-germacrene A (**7**) with relatively minor changes in k_{cat} and k_{cat}/K_m. By contrast, single H309 mutants gave rise to both (+)-germacrene A (**7**) and protoilludene (**8**) in addition to pentalenene (**2**). Mutation to glutamate of each of the three aspartate residues in the Mg^{2+}-binding aspartate-rich domain, ^{80}DDLFD, resulted in reduction in the k_{cat}/K_m for farnesyl diphosphate and formation of varying proportions of pentalenene and (+)-germacrene A (**7**). Formation of (+)-germacrene A (**7**) by the various pentalenene synthase mutants is the result of a derailment of the natural anti-Markovnikov cyclization reaction, and not simply the consequence of trapping of a normally cryptic, carbocationic intermediate. Both the N219A and N219L mutants of pentalenene synthase were completely inactive, while the corresponding N219D mutant had a k_{cat}/K_m which was 3300-fold lower than that of the wild-type synthase, and produced a mixture of pentalenene (**2**) (91%) and the aberrant cyclization product β-caryophyllene (**9**) (9%). Finally, the F77Y mutant had a k_{cat}/K_m which was reduced by 20-fold compared to that of the wild-type synthase.

Sesquiterpene synthases are a remarkably versatile family of enzymes that catalyze the cyclization of a single acyclic precursor, farnesyl diphosphate (**1**, FPP), to any of 300 known sesquiterpene hydrocarbons or alcohols.[1] The closely related monoterpene synthases cyclize geranyl diphosphate (GPP), the C_{10} acyclic homologue of FPP, to a variety of monocyclic and bicylic monoterpenes, using variations of the same ionization−cyclization mechanism.[2] The enzymes do not require any organic or inorganic cofactor other than a divalent cation, with Mg^{2+} or, in some cases, Mn^{2+} usually being preferred. The proteins themselves are usually monomers, or occasional homodimers, with subunit molecular weights of 40−65 kDa. Each multistep cyclization reaction normally takes place within a single active site without release of free intermediates.

Pentalenene synthase is a typical sesquiterpene synthase that catalyzes the Mg^{2+}-dependent cyclization of farnesyl diphosphate (**1**) to pentalenene (**2**),[3] the parent sesquiterpene hydrocarbon[4] of the pentalenolactone antibiotics, a family of metabolites which have been isolated from several species of Streptomycetes[5] (Scheme 1). The enzyme from *Streptomyces* UC5319, a monomer of 38 kDa, has been purified to homogeneity, cloned, and overexpressed in *Escherichia coli*.[6] The mechanism of the cyclization, which has been extensively studied using a variety of stereospecifically labeled forms of

Scheme 1

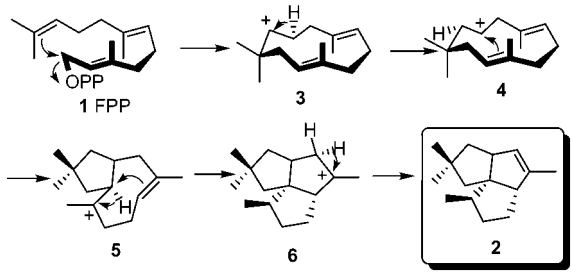

* To whom correspondence should be addressed. E-mail: David_Cane@brown.edu.
[†] Brown University.
[§] Wageningen Agricultural University and Plant Research International.
[‡] University of Pennsylvania.

(1) Cane, D. E. In *Isoprenoids Including Carotenoids and Steroids*; Cane, D. E., Ed. (Volume 2 in *Comprehensive Natural Products Chemistry*; Barton, D, Nakanishi, K., Meth-Cohn, O., Eds.); Pergamon Press: Elsevier: Oxford, 1999; pp 155−215.
(2) Croteau, R. B. In *Isoprenoids Including Carotenoids and Steroids*; Cane, D. E., Ed. (Volume 2 in *Comprehensive Natural Products Chemistry*; Barton, D, Nakanishi, K., Meth-Cohn, O., Eds.); Pergamon Press: Elsevier: Oxford, 1999; pp 97−153.
(3) Cane, D. E.; Tillman, A. M. *J. Am. Chem. Soc.* **1983**, *105*, 122−124. Cane, D. E.; Abell, C.; Tillman, A. M. *Bioorg. Chem.* **1984**, *12*, 312−328.
(4) Seto, H.; Yonehara, H. *J. Antibiot.* **1980**, *33*, 92−93.
(5) (a) Martin, D. G.; Slomp, G.; Mizsak, S.; Duchamp, D. J.; Chidester, C. G. *Tetrahedron Lett.* **1972**, 4901−4904. (b) For examples and leading references, see: Cane, D. E.; Sohng, J. K.; Williard, P. G. *J. Org. Chem.* **1992**, *57*, 844−852.
(6) Cane, D. E.; Sohng, J. K.; Lamberson, C. R.; Rudnicki, S. M.; Wu, Z.; Lloyd, M. D.; Oliver, J. S.; Hubbard, B. R. *Biochemistry* **1994**, *33*, 5846−5857.

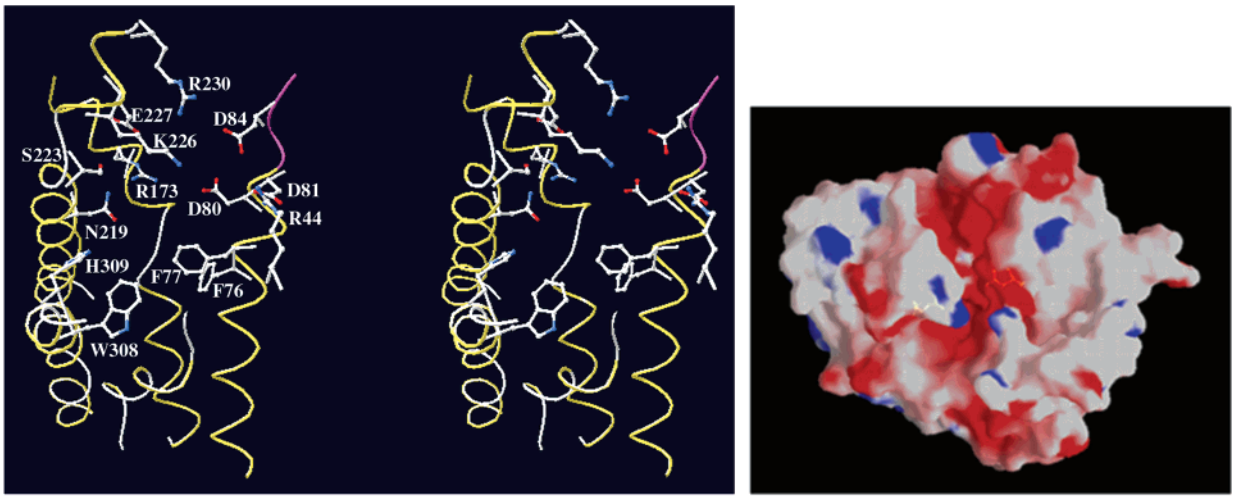

Figure 1. (A) Crossed-eye stereoview of pentalenene synthase active site, illustrating key active site residues. Polar residues at the top are believed to be involved in binding of Mg^{2+} and the pyrophosphate moiety of the FPP substrate, while aromatic residues deeper in the active site cleft provide a hydrophobic surface for the farnesyl residue and stabilize carbocation intermediates. View is from the side, with opening of active site at the top of the figure. (Generated by Swiss Pdb-Viewer.[38]) (B) Electrostatic surface of pentalenene synthase generated using GRASP.[39] Red regions indicate negative charge, and blue indicates positive charge. View is from the top of the active site cavity, with the aspartate-rich domain on the right.

FPP,[3,7] is believed to involve initial ionization of the pyrophosphate moiety followed by attack of the resulting allylic cation at C-11 of the distal double bond to give the humulyl cation **3** (Scheme 1). Rearrangement of **3** to the isomeric humulyl cation **4**, either by a 1,2-hydride shift or by a deprotonation−reprotonation sequence, is followed by cyclization to the seco-illudyl cation **5**. Hydride shift, cyclization, and stereospecific removal of the H-7*re* proton from the penultimate tricyclic intermediate **6** yields pentalenene. The cyclization is prototypical of all sesquiterpene cyclizations.

With the availability of numerous cloned sesquiterpene and monoterpene synthases, the role of each cyclase in catalyzing the formation of its characteristic terpenoid product has been the object of considerable speculation and intensive study. In each case, the cyclase protein is believed to bind and fold the acyclic substrate FPP (or GPP) in a specific conformation and to initiate cyclization by ionization of the allylic diphosphate moiety, assisted by Mg^{2+} or another divalent cation. Crystal structures of four different sesquiterpene cyclases—pentalenene synthase from the Gram-positive bacterium *Streptomyces* UC5319, trichodiene synthase and aristolochene synthase from the filamentous fungi *Fusarium sporotrichioides* and *Penicillium roqueforti*, respectively, and epi-aristolochene synthase from the tobacco plant, *Nicotiana tabacum*[8]—have indicated a remarkably high degree of conservation in the three-dimensional structures of all synthases, despite an essentially complete lack of overall amino acid sequence similarity among any of these proteins.[9] This conserved topology, which consists entirely of α-helices connected by short peptide loops, has been termed the class I α-helical terpenoid cyclase fold.[8c] Interestingly, the same fold is also observed for avian farnesyl diphosphate synthase[10] and human squalene synthase,[11] two enzymes which catalyze mechanistically analogous reactions of allylic diphosphate substrates. The active sites of all of these enzymes consist of a conical and hydrophobic active site cleft, flanked by six or seven helices and lined with an unusual number of aromatic and nonpolar amino acid residues (Figure 1A). In the case of pentalenene synthase, the cleft is approximately 9 Å wide and 15 Å deep.[8a] The aromatic side chains are thought to play a critical role in shaping the active site and specifically stabilizing the succession of carbocationic intermediates that are generated in the course of each cyclization.[12] Stabilization of the carbocations is further enhanced by the negative electrostatic charge of the interior surface of the active site (Figure 1B). Near the upper edge of the active site cavity of each synthase, located at the C-terminal end of an α-helix, is a universally conserved aspartate-rich motif, DDXXD, that has been implicated in the binding of the pyrophosphate moiety of the substrate through chelation of the requisite divalent cation.[1,2,10,13,14] On the

(7) Cane, D. E.; Oliver, J. S.; Harrison, P. H. M.; Abell, C.; Hubbard, B. R.; Kane, C. T.; Lattman, R. *J. Am. Chem. Soc.* **1990**, *112*, 4513−4524. Cane, D. E.; Weiner, S. W. *Can. J. Chem.* **1994**, *72*, 118−127. Cane, D. E.; Abell, C.; Harrison, P. H.; Hubbard, B. R.; Kane, C. T.; Lattman, R.; Oliver, J. S.; Weiner, S. W. *Philos. Trans. R. Soc. B* **1991**, *332*, 123−129.

(8) (a) Pentalenene synthase: Lesburg, C. A.; Zhai, G.; Cane, D. E.; Christianson, D. W. *Science* **1997**, *277*, 1820−1824. (b) Trichodiene synthase: Rynkiewicz, M. J.; Cane, D. E.; Christianson, D. W. *Proc. Natl. Acad. Sci. U.S.A.* **2001**, *98*, 13543−13548. Rynkiewicz, M. J.; Cane, D. E.; Christianson, D. W. *Biochemistry* **2002**, *41*, 1732−1741. (c) Aristolochene synthase: Caruthers, J. M.; Kang, I.; Rynkiewics, M. J.; Cane, D. E.; Christianson, D. *J. Biol. Chem* **2000**, *275*, 25533−25539. (d) Epi-aristolochene synthase: Starks, C. M.; Back, K.; Chappell, J.; Noel, J. P. *Science* **1997**, *277*, 1815−1820.

(9) Although sesquiterpene synthases of microbial origin generally show no significant overall sequence similarity either to one another or to any other class of proteins (except for orthologs biosynthesizing the same sesquiterpene product), the dozens of known monoterpene, sesquiterpene, and diterpene synthases from plant sources have strongly conserved primary amino acid sequences as well as a common intron organization and exon size, consistent with a common evolutionary origin (cf.: Trapp, S. C.; Croteau, R. B. *Genetics* **2001**, *158*, 811−832.) It is highly likely, therefore, that all such plant terpene synthases will have the same topology as epi-aristolochene synthase.

(10) Tarshis, L. C.; Yan, M. J.; Poulter, C. D.; Sacchettini, J. C. *Biochemistry* **1994**, *33*, 10871−10877. Tarshis, L. C.; Proteau, P. J.; Kellogg, B. A.; Sacchetini, J. C.; Poulter, C. D. *Proc. Natl. Acad. Sci. U.S.A.* **1996**, *93*, 15018−15203.

(11) Pandit, J.; Danley, D. E.; Schulte, G. K.; Mazzalupo, S.; Pauly, T. A.; Hayward, C. M.; Hamanaka, E. S.; Thompson, J. F.; Harwood, H. J., Jr. *J. Biol. Chem.* **2000**, *275*, 30610−30617.

(12) (a) Dougherty, D. A. *Science* **1996**, *271*, 163−168. (b) Lesburg, C. A.; Caruthers, J. M.; Paschall, C. M.; Christianson, D. W. *Curr. Opin. Struct. Biol.* **1998**, *8*, 695−703.

(13) Ashby, M. N.; Edwards, P. A. *J. Biol. Chem.* **1990**, *265*, 13157−13164.

Table 1. Pentalenene Synthase Mutants

mutant	plasmid	steady-state kinetic parameters			relative proportion of sesquiterpenes (%)			
		k_{cat} (s^{-1})	K_m (μM)	k_{cat}/K_m (s^{-1} M^{-1})	**2**	**7**	**8**	**10**
WT PS	pZW05	0.3	0.3	1.0×10^6	100	0	0	0
H309A	pGZ11	0.11	0.19	0.6×10^6	78	10	12	0
H309S	pGZ12	0.11	0.25	0.4×10^6	82	10	8	0
H309C	pGZ13	0.07	0.33	0.2×10^6	80	13	7	0
H309F	pMS11	0.018	1.43	1.2×10^4	84	13	3	0
W309F/H309F	pMS03	0.025	0.61	4.1×10^4	62	25[a]	0	0
W309F	pMS04	0.074	0.16	4.6×10^5	93	7	0	0
D80E	pMS05	0.002	6.98	286	100	0	0	0
D81E	pMS06	0.0065	2.6	2500	92	4.5[b]		0
D84E	pMS08	0.81	2.28	0.35×10^6	97	3		0
F77Y	PMS09	0.016	0.3	5.2×10^4	>97	0	0	0
N219A	pGZ14			inactive				
N219L	pGZ17			inactive				
N219D	pMS07	0.005	16.6	3.0×10^2	91	0	0	9

[a] The W308F/H309F mutant also produced an additional 13% of a 1:1 mixture of two unidentified hydrocarbons, *m*/*z* 204. [b] The D81E mutant also produced 3.5% of an unidentified hydrocarbon, *m*/*z* 204.

Scheme 2

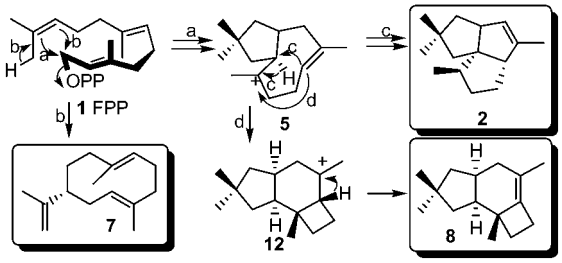

opposite wall is found another highly conserved triad of amino acid side chains, (**D/N**)DXX(**S/T**)XXX**E**, that also plays an important role in Mg^{2+} binding[8b,d,15] (Figure 1A). Despite the increasing amount of structural information, little is known about the precise manner by which pentalenene synthase and related terpene cyclases impose a specific conformation on their acyclic, lipophilic substrates or trigger the ionization of the allylic diphosphate, how they mediate the resultant cascade of electrophilic reactions, or how they determine the timing and stereochemistry of the quenching of the carbocationic intermediates, either by removal of a specific proton or by capture by an external nucleophile such as water.

In the crystal structure of pentalenene synthase, the only apparent basic residue in the active site cavity is histidine-309[8a] (Figure 1A). Modeling of both FPP and derived intermediates into the active site originally led us to suggest that the imidazole side chain of H309 might serve as the functional active site base that mediates the postulated series of deprotonations and reprotonations, including the final deprotonation that generates pentalenene. This inference was firmly excluded, however, when site-directed mutagenesis showed that H309 is not required for catalytic activity.[16] Indeed, the H309A, H309C, H309S, and H309F mutants all retained substantial pentalenene synthase activity, with relatively minor decreases in k_{cat} ranging from as little as 3-fold for H309A and H309S to at most ~17-fold for the H309F mutant, accompanied by only minor increases in K_m for three of the mutants (Table 1). On the other hand, each of these mutants was found to produce up to 20% of varying proportions of two sesquiterpene hydrocarbons which we identified as germacrene A (**7**) and protoilludene (**8**)[16] (Scheme 2). Both of these latter compounds result from derailment of the normal cyclization cascade, presumably due to relaxed control over the conformations of the substrate FPP and the derived carbocationic intermediates in the active sites of the various H309 mutants. We now report the results of site-directed mutagenesis of additional active site residues that shed light on the mechanism of action of pentalenene synthase.

Results

Active Site Base. Having ruled out H309 as the active site base, we turned our attention to other plausible amino acid candidates. Unfortunately, no other nominally basic amino acids are present in the active site. The various arginine and lysine residues (R157, R173, K226, and K230) which are present along the upper region of the active site cavity are expected to be present in their protonated, positively charged form and are thought to play a role in binding of the pyrophosphate moiety of the substrate, rather than as Lewis bases. We therefore had to consider other, less conventional, possibilities. A tryptophan residue has previously been suggested as a possible active site base for epi-aristolochene synthase.[8d] Noting that pentalenene synthase also has a tryptophan residue (W308) immediately adjacent to the previously examined H309 (Figure 1A), we generated two pentalenene synthase mutants in which this tryptophan was replaced by phenylalanine, W308F, and the double mutant W308F/H308F (Table 1). Each of these mutant proteins was purified to homogeneity, and the steady-state kinetic parameters were determined, as previously described for the wild-type recombinant synthase. Both mutants retained substantial pentalenene synthase activity, with k_{cat} lowered by a factor of only 4−12 and an overall reduction in k_{cat}/K_m of between 2 and 25. Interestingly, the W308F/H309F double mutant was actually slightly more active than the single H309F mutant. Unlike the simple H309 mutants, however, neither W308 mutant produced detectable protoilludene (**8**). Instead, the W308F and W308F/H309F mutants generated a mixture of pentalenene (**2**) and 7% and 25% of (+)-germacrene A (**7**), respectively, with the double mutant producing an additional 13% of equal quantities of two as-yet unidentified sesquiterpene hydrocarbons. The absolute configuration of the enzymatically generated (+)-germacrene A (**7**) was established by means of its facile Cope rearrangement to (−)-β-elemene (**9**), a reaction

(14) Cane, D. E.; Xue, Q.; Fitzsimons, B. C. *Biochemistry* **1996**, *35*, 12369−12376.
(15) Cane, D. E.; Kang, I. *Arch. Biochem. Biophys.* **2000**, *376*, 354−364.
(16) Portions of this work dealing with the H309A, H309S, H309C, and H309F mutants have been published in preliminary form. For details of the identification of **7** and **8**, see: Seemann, M.; Zhai, G.; Umezawa, K.; Cane, D. *J. Am. Chem. Soc.* **1999**, *121*, 591−592.

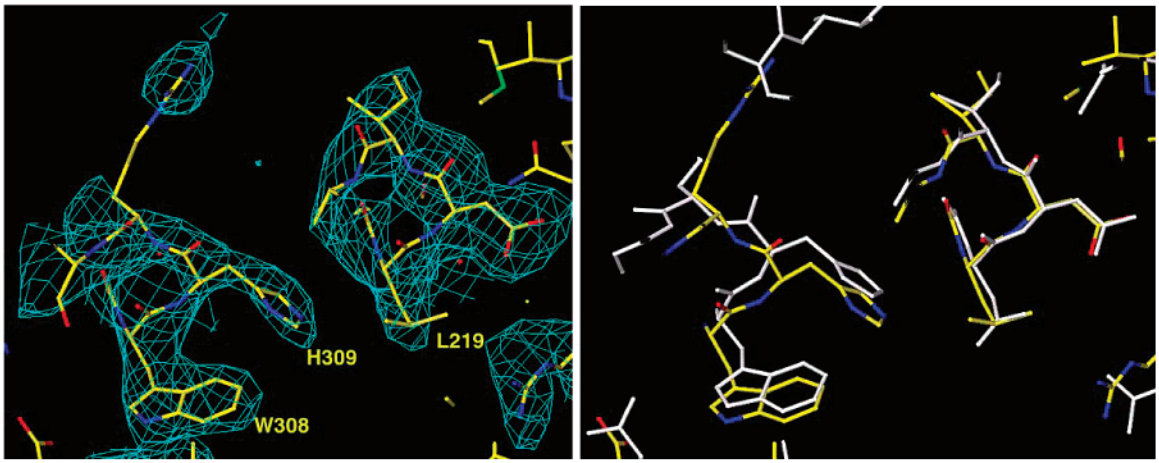

Figure 2. (A) Difference electron density map calculated with Fourier coefficients $|F_o| - |F_c|$ and phases calculated from the final model less the atoms of the three indicated residues and all atoms within a 2 Å radius of them, contoured at 2σ. The substituted L219 side chain is indicated along with other active site residues. (B) Least-squares superposition of N219L pentalenene synthase (yellow) and wild-type pentalenene synthase (white) active sites (orientation is the same as in panel A). Note that the N219L substitution is accommodated without significant structural changes in the enzyme active site.

Scheme 3

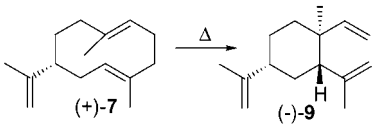

which occurs with retention of configuration at C-7, the site of the 2-propenyl substituent[17] (Scheme 3). The (−)-β-elemene (**9**) produced in each rearrangement was identified by direct comparison with an authentic (−)-β-elemene standard by chiral capillary GC−MS.[18] All of the previously described single H309 mutants were also shown to produce (+)-germacrene (**7**).

Aspartate-Rich Domain. To explore the role of the aspartate-rich domain of pentalenene synthase, each of the three aspartate residues was separately replaced by a glutamate. The D80E mutant suffered a 150-fold decrease in k_{cat} as well as a more than 20-fold increase in K_m, resulting in a net decrease in k_{cat}/K_m of $\sim 3.5 \times 10^3$ (Table 1). Interestingly, despite the substantial reduction in catalytic efficiency compared to the efficiency of the wild-type synthase, the sole product generated by the D80E mutant was pentalenene. By contrast, the D81E mutant, which exhibited a 400-fold reduction in k_{cat}/K_m compared to the wild type's value, due to a combination of a nearly 50-fold decrease in k_{cat} and a 9-fold increase in K_m, generated a mixture of 92% pentalenene and 4.5% germacrene A (**7**), accompanied by an additional 3.5% of an as-yet unidentified sesquiterpene hydrocarbon, *m*/*z* 204. Finally, the D84E mutant, which displayed relative minor changes in steady-state parameters (2.5-fold increase in measured k_{cat} offset by a 7-fold increase in K_m), generated a 97:3 mixture of pentalenene and **7**.

Asparagine-219. We have previously noted that the side chain of asparagine-219 protrudes into the active site cavity of pentalenene synthase[8a] (Figure 1A). Originally, we had proposed that this residue might influence the cyclization reaction, by enforcing a specific folding on the substrate, FPP, and possibly by stabilizing transient cations by dipole−cation interactions. Structural studies of both epi-aristolochene synthase[8d] and trichodiene synthase,[8b] however, suggest that the carbonyl oxygen of the side chain amide of N219 in pentalenene synthase is part of a highly conserved Mg^{2+}-binding triad that also includes the side chain oxygen atoms of serine-223 and glutamate-227. Accordingly, we generated both the isosteric N219L mutant and the corresponding N219A mutant (Table 1). Significantly, each of these mutants was completely inactive, within the limits of detection of the assay, which could have measured a reduction in k_{cat} of as much as a factor of 10^5.

To probe further the structural basis for the loss of activity associated with replacement of N219, and to verify that the loss of activity of the N219L mutant was not due to loss of structural integrity of the pentalenene synthase active site, we solved the crystal structure of the N219L mutant and compared it to that of the wild-type pentalenene synthase. Attempts to also obtain crystals of the N219L mutant with bound FPP were unsuccessful. The electron density map of N219L pentalenene synthase, shown in Figure 2A, reveals clear electron density for the substituted leucine side chain. Moreover, the superposition of N219L pentalenene synthase with wild-type pentalenene synthase, illustrated in Figure 2B, reveals that the nominally isosteric amino acid substitution does not result in any significant conformational changes for neighboring residues in the enzyme active site, indicating that the active site contour appears to be conserved in the mutant despite the replacement of the neutral but polar side chain of N219 with the hydrophobic leucine residue.[8a]

Overall, the final refined structure of N219L pentalenene synthase at 2.9 Å is very similar to that of the wild-type enzyme (Figures 2B and 3). There are, however, some minor but interesting differences in the upper active site region when the two structures are compared. In the wild-type pentalenene synthase structure, the F158-D164 polypeptide loop connecting helices F and G at the rim of the active site is disordered in both monomers, A and B, of the asymmetric unit.[8a] In monomer A of the N219L mutant, this polypeptide loop is similarly

(17) Takeda, K. *Tetrahedron* **1974**, *30*, 1525−1534. Weinheimer, A. J.; Youngblood, W. W.; Washecheck, P. H.; Karns, T. K. B.; Ciereszko, L. S. *Tetrahedron Lett.* **1970**, *7*, 497−500.
(18) König, W. A.; Rieck, A.; Hardt, I.; Gehrcke, B.; Kubeczka, K.-H.; Muhle, H. *J. High Resolut. Chromatogr.* **1994**, *17*, 315−320. De Kraker, J.-W.; Franssen, M. C. R.; de Groot, A.; König, W. A.; Bouwmeester, H. J. *Plant Physiol.* **1998**, *117*, 1381−1392.

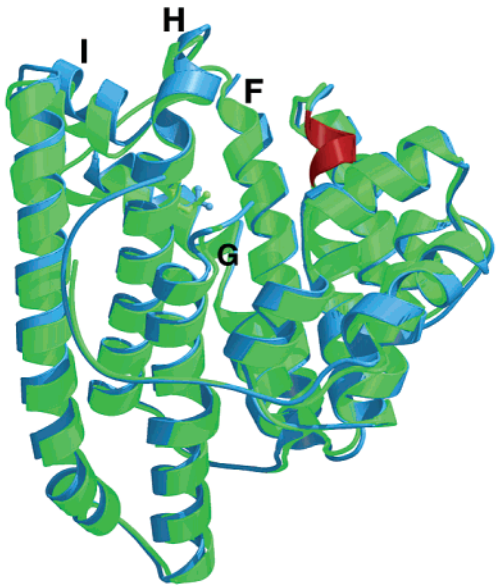

Figure 3. Least-squares ribbon-plot superposition of N219L pentalenene synthase (green) and wild-type pentalenene synthase (blue) generated with MOLSCRIPT[40] and Raster3D.[41] Helices F, G (partially hidden), H, and I are indicated; N219 in the wild-type and the substitute amino acid side chain, L219, are shown on helix H. The aspartate-rich region is red in both structures.

disordered, while in monomer B, the corresponding polypeptide loop is fully ordered in the electron density map. As a consequence, segmental shifts of α-helical segments in the region of this loop are evident in the superposition of monomers B in the wild-type pentalenene synthase and N219L mutant structures: 1−2 Å segmental shifts are greatest for the upper part of helices G and H (starting at the site of the N219L substitution on helix H) and for all of helix I (Figure 3). Although it is likely that these structural changes occur in monomer B as a consequence of the N219L substitution on helix H, it is not clear why these structural changes are observed only in monomer B of the asymmetric unit and not in monomer A of the mutant. Neither the wild-type protein nor the N219L mutant shows any bound Mg^{2+}, similar to free aristolochene synthase[8c] and trichodiene synthase,[8b] but in contrast to epi-aristolochene synthase.[8d]

The majority of plant sesquiterpene and monoterpene synthases have an aspartate instead of an asparagine in the conserved Mg^{2+}-binding triad at the position corresponding to N219 of pentalenene synthase. Reasoning that some or all of the original cyclase activity might be retained when asparagine was replaced with aspartate, we also prepared the N219D mutant. The latter variant indeed showed pentalenene synthase activity, albeit at a lower level than wild-type, with a 60-fold decrease in k_{cat} and a 55-fold increase in the K_m for FPP, resulting in a ca. 3300-fold decrease in k_{cat}/K_m. Intriguingly, the N219D mutant produced 9% of a new hydrocarbon which was shown to be identical by GC−MS with an authentic sample of β-caryophyllene (**10**) (Scheme 4). Neither of the previously observed derailment products, **7** or **8**, were observed in incubations with N219D. The formation of β-caryophyllene (**10**) is readily explained by an alternative cyclization of the normal humulyl cation intermediate **3** and removal of a proton from the methyl group of the resulting bicyclic cation **11**.

Aromatic Residues. Among the many aromatic residues which line the active site of pentalenene synthase, two of these,

Scheme 4

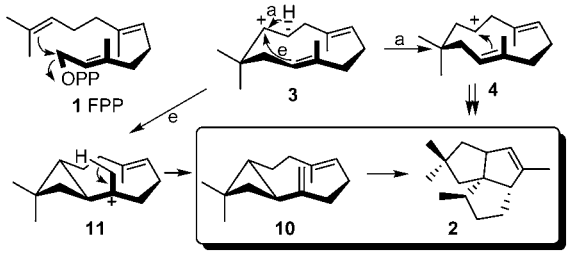

phenylalanines-76 and -77, are found on helix D, immediately below the aspartate-rich domain, with the faces of the phenyl rings angled toward the active site in a sort of open-faced sandwich (Figure 1A). Although both the F76A and F77A mutants were constructed, the resultant proteins were obtained in low yield and primarily as insoluble inclusion bodies, even when lower temperatures and reduced concentrations of IPTG were used for induction of protein expression. On the basis of experiments with partially purified soluble components of each mutant extract, the activity of each mutant was estimated as no more than 10% that of the wild-type enzyme, and probably considerably less. Attempted solubilization and refolding of the F76A mutant gave only inactive protein. On the other hand, the F77Y mutant was readily expressed and purified in soluble form. The k_{cat} and the k_{cat}/K_m of the F77Y mutant were 20-fold lower than those of the wild-type pentalenene synthase (Table 1). The latter mutant produced predominantly pentalenene (**2**), along with very minor amounts of as-yet unidentified sesquiterpene hydrocarbons, none of which corresponded to either germacrene A or protoilludene.

Discussion

Active Site Base. In the crystal structure of pentalenene synthase, the only apparent basic residue in the active site cavity is histidine-309[8a] (Figure 1A). This observation originally led us to suggest that the imidazole side chain of H309 might serve as the functional active site base, an inference which was firmly excluded, however, when site-directed mutagenesis showed that His309 is not required for catalytic activity.[16] Although the H309A, H309C, H309S, and H309F mutants all retained substantial pentalenene synthase activity, each of these mutants was found to produce up to 20% of varying proportions of two sesquiterpene hydrocarbons identified as (+)-germacrene A (**7**) and protoilludene (**8**). The formation of protoilludene (**8**) by each of these mutants is readily explained by direct cyclization of the natural seco-illudyl cation intermediate **5** followed by deprotonation of the resulting tricyclic protoilludyl cation (**12**) (Scheme 2). Protoilludene (**8**) has previously been isolated from cultures of *Fomitopsis insularis* that produce the structurally related sesquiterpene fomannosin.[19] Formation of germacrene A (**7**) requires an anomalous Markovnikov cyclization of the originally generated allylic cation at C-10 of the 10,11-double bond of FPP, followed by deprotonation of one of the two attached methyl groups (Scheme 2). Germacrene A (**7**) is itself a common sesquiterpene metabolite that has also been implicated as an intermediate in the formation of a wide variety of bicyclic eudesmane, eremophilane, and vetispirane sesquiterpenes, including both aristolochene and epi-aristolochene.[1,18,20] Notably, the formation of the (+)-enantiomer of **7** is consistent with the

(19) Furukawa, J.; Morisaki, N.; Kobayashi, H.; Iwasaki, S.; Nozoe, S.; Okuda, S. *Chem. Pharm. Bull.* **1985**, *33*, 440−443.

well-documented absolute sense of folding of FPP in the formation of pentalenene. Both anomalous cyclization products, (+)-germacrene A (**7**) and protoilludene (**8**), result from derailment of the normal cyclization cascade, presumably due to relaxed control over the conformation of the substrate FPP and derived intermediates in the active sites of the various H309 mutants.

In their analysis of the structure of epi-aristolochene synthase, Chappell and Noel had postulated that an active site tryptophan (W273) might serve as a Lewis base, reasoning that the indole ring is intrinsically reactive toward acid and other electrophilic reagents.[8d,21] In support of this suggestion, they reported that replacement of W273 by either aromatic or nonaromatic amino acid residues abolished cyclase activity in the epi-aristolochene synthase. Since pentalenene synthase has a tryptophan residue (W308) immediately adjacent to the previously examined His309, we generated two mutant pentalenene synthases in which this tryptophan was replaced by phenylalanine, W308F, and the double mutant, W308F/H308F (Table 1). Both mutants retained substantial pentalenene synthase activity. Although neither mutant produced detectable protoilludene (**8**), the W308F and W308F/H309F mutants also generated varying proportions of (+)-germacrene A (**7**). Together these experiments firmly exclude either histidine-309 or tryptophan-308 as the active site base for pentalenene synthase.

Deprotonation of the carbocationic intermediates of terpenoid cyclization does not require an especially potent base, since tertiary carbocations are highly acidic, with estimated pK_a values in the range of -10.[22] The *stereospecific* removal of H-7*re* of **6** that generates pentalenene (**2**) is certainly not a spontaneous chemical event and is presumably mediated by a discrete, dedicated active site base. It is geometrically unlikely, however, that this same base can also mediate each of the anomalous deprotonations that generate the various derailment products such as germacrene A, protoilludene, and β-caryophyllene. Since we have ruled out the only nominally basic residues present in the active site, His309 and the adjacent Trp308, as active site bases, how can one now account for the action of apparently multiple bases? At least three possibilities must be considered: (1) The base or bases could be enzyme-bound water(s), given that the pK_a of the conjugate acid H_3O^+ is -2 to -4.[22] A potential drawback to water acting as the active site base, however, is its intrinsic nucleophilicity, which could lead to the competing formation of alcohol side products, none of which are observed for either the wild-type cyclase or any of the mutants examined. In principle, this nucleophilicity could be suppressed if the bound water were to be tightly constrained within the active site. So far, there is no crystallographic evidence for or against the presence of water bound at the active site in the presence of substrates or analogues. (2) The carbonyl oxygen atoms of the peptide backbone are also basic enough (pK_a of protonated amide = 0 to -2)[22] to accept a proton from the C-7 methylene group of **6** and other cationic intermediates. (3) Finally, the active site base might be the tightly bound pyrophosphate counterion.[23] It is not immediately clear, however, that this group would be capable of reaching all of the various sites of deprotonation that lead to the formation of pentalenene and its three identified derailment products. Resolution of these issues will require high-resolution crystal structures of protein bound to substrate or intermediate analogues.

Binding of the Divalent Cation. The aspartate-rich domain, which is universally conserved in all terpene synthases, has been shown to play an important role in binding of the requisite divalent cation, which is usually Mg^{2+}.[1,2,10,13,14] Crystal structures of both epi-aristolochene synthase with a bound FPP analogue,[8d] as well as of trichodiene synthase with bound inorganic pyrophosphate,[8b] have revealed that, in fact, three Mg^{2+} ions are bound at the active site, two of which are liganded, either directly or indirectly, by two or more of the carboxylates of the DDXXD motif. These two Mg^{2+} ions in turn form a complex with the pyrophosphate moiety of the substrate. Together with a third magnesium ion, which is held on the opposite side of the pyrophosphate group by the (**N/D**)-DXX(**S/T**)XXX**E** triad of amino acid side chains, the divalent metal ions serve to bind and orient the pyrophosphate group of the substrate FPP, while simultaneously activating the allylic diphosphate moiety for the ionization that initiates the cascade of electrophilic cyclization reactions. Consistent with this model, replacement of the individual aspartate residues in each of two aspartate-rich domains in the active site of farnesyl diphosphate synthase resulted in nearly complete loss of prenyl transferase activity.[24] By contrast, the corresponding D100E, D101E, and D104E mutants of trichodiene synthase display only modest changes in steady-state kinetic parameters (but up to 100-fold decreases in the slowest chemical step, that of FPP ionization), while generating a mixture of five anomalous sesquiterpene cyclization products in addition to the normal cyclization product, trichodiene.[14] Recent crystallographic studies of the D100E mutant of trichodiene synthase with bound inorganic pyrophosphate have revealed that the complex coordinates only two of the three Mg^{2+} ions and that the volume of the active site cavity has increased some 12%, from 324 to 364 Å^3, allowing for greater spatial and conformational degrees of freedom in the binding of the substrate and derived intermediates.[8b] For pentalenene synthase, the D80E, D81E, and D84E mutants also show an analogous degradation in catalytic power and product specificity, although there is no simple correlation between the magnitude of the change in steady-state kinetic parameters and the relative proportions of abortive cyclization products. Since release of the final sesquiterpene products is likely to be rate-limiting, as has been demonstrated for both trichodiene synthase and epi-aristolochene synthase,[25] even a 10-fold decrease in the rate of the slowest chemical step in the pentalenene synthase reaction sequence could well be masked by an even slower product-off step.

Asparagine-219 of pentalenene synthase is part of a highly conserved motif, (L,V)(I,V,L)(**N**,**D**)D(I,L,V)A(**S**,**T**)XXX**E**, that

(20) Rising, K. A.; Starks, C. M.; Noel, J. P.; Chappell, J. *J. Am. Chem. Soc.* **2000**, *122*, 1861−1866. Cane, D. E.; Tsantrizos, Y. S. *J. Am. Chem. Soc.* **1996**, *118*, 10037−10040.

(21) Biswas, K. M.; Jackson, A. H. *J. Chem. Soc., Perkin Trans. 1* **1989**, *11*, 1981−1986. Abdullah, M. I.; Jackson, A. H.; Lynch, P. P.; Record, K. A. F. *Heterocycles* **1990**, *30*, 317−320.

(22) Deno, N. C. *Prog. Phys. Org. Chem.* **1964**, *2*, 129−193. Lowry, T. H.; Richardson, K. S. *Mechanism and Theory in Organic Chemistry*; Harper & Row: New York, 1976; pp 149−151. See also http://webbook.nist.gov/chemistry/

(23) Davisson, V. J.; Neal, T. R.; Poulter, C. D. *J. Am. Chem. Soc.* **1993**, *115*, 1235−1245.

(24) Marrero, P. F.; Poulter, C. D.; Edwards, P. A. *J. Biol. Chem.* **1992**, *267*, 21873−21878. Song, L. S.; Poulter, C. D. *Proc. Natl. Acad. Sci. U.S.A.* **1994**, *91*, 3044−3048.

(25) (a) Cane, D. E.; Chiu, H.-T.; Liang, P.-H.; Anderson, K. S. *Biochemistry* **1997**, *36*, 8332−8339. (b) Mathis, J. R.; Back, K.; Starks, C.; Noel, J.; Poulter, C. D.; Chappell, J. *Biochemistry* **1997**, *36*, 8340−8348.

is found in all monoterpene, sesquiterpene, and diterpene synthases.[15] Both N225 of trichodiene synthase[8b] and D445 of epi-aristolochene synthase,[8d] each of which is known to be chelated to a Mg^{2+} ion, are found at nearly identical positions within the active sites of their respective enzymes as N219 and N244 of pentalenene and aristolochene synthase, and all four residues have their side chain carbonyl groups oriented in the same manner. Consistent with the expected role of N219 in binding Mg^{2+}, the corresponding N219A and N219L mutants of pentalenene synthase are both completely inactive. Analysis of the crystal structure of the latter mutant reveals no significant changes in protein structure or in the shape of the active site (Figures 2 and 3). Notably, we have also recently found that the N244L mutant of aristolochene synthase is inactive, as predicted.[26] Croteau has recently reported that the homologous N765A mutant of abietadiene synthase, a diterpene synthase originally isolated from grand fir (*Abies grandis*), suffers a more than 20 000-fold decrease in k_{cat} compared to the value for the wild type, while substitution of alanine for either T769 or E773, the other two components of the Mg^{2+}-binding triad, reduced k_{cat} by 10 000-fold and 5000-fold, respectively.[27] On the other hand, replacement of N219 of pentalenene synthase with aspartate, the amino acid that is found at the homologous position of the majority of plant monoterpene, sesquiterpene, and diterpene synthases, restores pentalenene synthase activity to ca. 0.03% of its wild-type level, while resulting in concomitant formation of the anomalous side-product β-caryophyllene (**10**) (Scheme 4).

Carbocation Stabilization. Both theoretical and experimental studies have provided support for the importance of aromatic amino acid residues in stabilizing carbocations at enzyme active sites.[12] Among the many aromatic residues that can be seen within the active site of pentalenene synthase, F76 and F77 appear to be well placed so as to interact with positive charge at C-1, C-2, and C-3 of the farnesyl residue and derived intermediates (Figure 1A). Replacement of either F76 or F77 by alanine led to at least a 10-fold reduction in catalytic activity, but the low yield and poor solubility of the mutant proteins precluded more quantitative analysis of the steady-state kinetic parameters. Mutant F77Y, in which the phenylalanine is replaced by a more electron-rich tyrosine residue, produced predominantly pentalenene, with essentially no change in K_m compared to the value for the wild type but with k_{cat} reduced by a factor of 20, suggesting that the precise geometry of interaction of the aromatic residues with the intermediate carbocations is critical to enhancement of the rate of the reaction.

The currently accepted mechanism for the pentalenene synthase reaction involves ionization of the substrate FPP and electrophilic attack of C-1 of the initially generated allylic cation at C-11 of the 10,11-double bond of FPP to give the secondary humulyl cation **3** (Scheme 5, pathway a). This anti-Markovnikov regiochemistry contrasts with solution-phase reactions in which electrophilic additions normally occur at the less substituted end of a double bond to give the more highly substituted, thermodynamically more stable carbocation. In those mutants of pentalenene synthase in which (+)-germacrene A (**7**) is generated in addition to pentalenene, formation of **7** results from competing Markovnikov addition to C-10 of the 10,11-double

Scheme 5

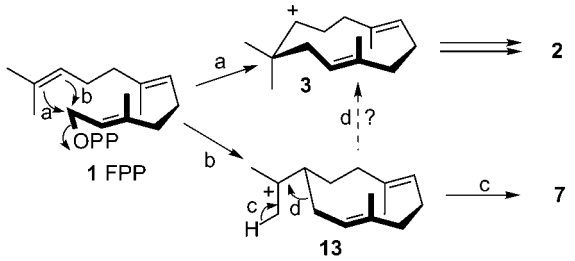

bond and deprotonation of the resulting tertiary cation **13** (Scheme 5, pathways b and c). Is formation and trapping of the germacradienyl cation **13** an anomalous process that occurs in competition with direct formation of the humulyl cation **3** only in pentalenene synthase mutants in which the substrate is anomalously bound, or is the germacradienyl cation **13** a natural, but normally cryptic, intermediate of the wild-type cyclization reaction, that ordinarily undergoes rapid Wagner−Meerwein rearrangement (Scheme 5, pathway d) to the secondary humulyl cation **3**?

The apparent selective formation of the nominally less stable, anti-Markovnikov addition product is, in fact, a very common theme in the biosynthesis of cyclic terpenoids, from monoterpenes to triterpenes.[1,2,28] This apparent divergence from ordinary solution or gas-phase kinetic behavior has motivated a variety of proposals to account for the apparently divergent chemistry of enzyme-catalyzed terpene synthase reactions. For example, on the basis of extensive studies of the cyclization of heteroatom-substituted squalene analogues by lanosterol synthase, Corey and others have argued that, in the generation of ring C of steroids and other triterpenes, the apparent direct, anti-Markovnikov cyclization of the bicyclic intermediate **14** leading to the formation of the tricyclic secondary cation **15** (Figure 4A, pathway a) can be avoided if one posits an initial Markovnikov cyclization of **14** to generate the tertiary cyclopentylcarbinyl cation **16**[29] (Figure 4A, pathway b). The latter intermediate would then undergo ring expansion to generate the secondary cyclohexyl cation **15** (Figure 4A, pathway c). Detailed calculations carried out by Jorgensen, using both ab initio and molecular mechanics methods to model the cyclization−rearrangement in a condensed phase designed to mimic the environment of aromatic residues thought to be at the active site of lanosterol synthase, predicted that direct Markovnikov cyclization of **14** to **16** would be exothermic by > -8 kcal/mol, while subsequent rearrangement of **16** to the secondary cation **15** would be endothermic by 12 kcal/mol.[30] These results were interpreted as being consistent with the cyclization−rearrangement pathway proposed by Corey. On the other hand, since the free energy of the ultimately formed secondary cation **15** cannot depend on the pathway by which it is formed, generation of **15** from the hypothetical Markovnikov intermediate **16** must be at least 8 kcal/mol *more endothermic* than direct

(26) Felicetti, B.; Cane, D. E. Unpublished observations.
(27) Peters, R. J.; Croteau, R. B. *Proc. Natl. Acad. Sci. U.S.A.* **2002**, *99*, 580−584.
(28) Abe, I.; Prestwich, G. D. In *Isoprenoids Including Carotenoids and Steroids*; Cane, D. E., Ed. (Volume 2 in *Comprehensive Natural Products Chemistry*; Barton, D, Nakanishi, K., Meth-Cohn, O., Eds.); Pergamon Press: Elsevier: Oxford, 1999; pp 267−298. Poralla, K. In *Isoprenoids Including Carotenoids and Steroids*; Cane, D. E., Ed. (Volume 2 in *Comprehensive Natural Products Chemistry*; Barton, D, Nakanishi, K., Meth-Cohn, O., Eds.); Pergamon Press: Elsevier: Oxford, 1999; pp 299−319.
(29) Corey, E. J.; Virgil, S. C.; Cheng, H. M.; Baker, C. H.; Matsuda, S. P. T.; Singh, V.; Sarshar, S. *J. Am. Chem. Soc.* **1995**, *117*, 11819−11820. Wendt, K. U.; Schulz, G. E.; Corey, E. J.; Liu, D. R. *Angew. Chem., Int. Ed.* **2000**, *39*, 2812−2833.
(30) Jenson, C.; Jorgensen, W. L. *J. Am. Chem. Soc.* **1997**, *119*, 10846−10854.

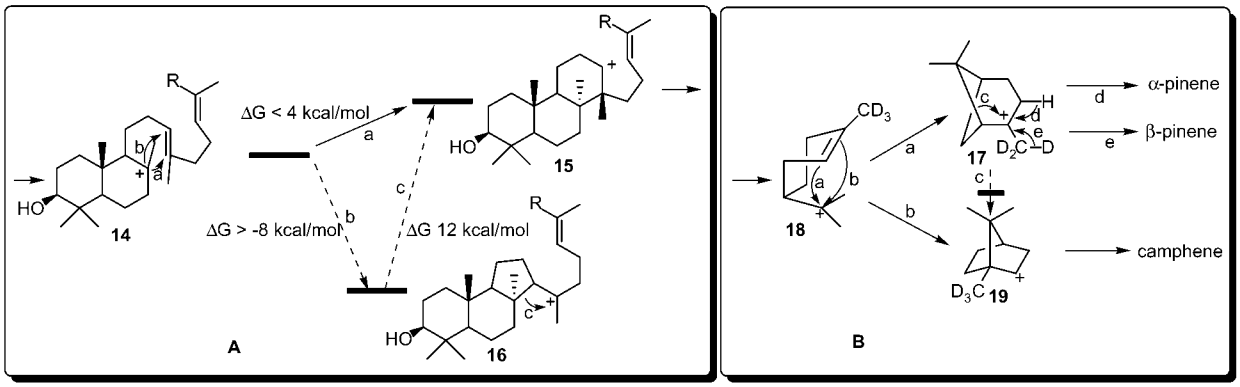

Figure 4. (A) Markovnikov (b) versus anti-Markovnikov (a) cyclization of the lanosterol precursor **14**. (B) Competing Markovnikov (a) and anti-Markovnikov (b) cyclization of the α-terpinyl cation **18** in the formation of α-pinene, *β*-pinene, and camphene by pinene synthase.

generation of **15** from **14** by the supposedly forbidden anti-Markovnikov process. In fact, the calculations themselves show the tricyclic secondary cation **15** to be no more than 4 kcal/mol higher in free energy than the bicyclic precursor **14**, most of the driving force for the reaction coming from the net conversion of a double bound to a single bond. There is thus no direct experimental evidence or theoretical support for an intrinsic thermodynamic (or, more importantly, kinetic) advantage to the proposed two-step cyclization−rearrangement process; indeed, such a pathway would require a thermodynamically *unfavorable* rearrangement step after the hypothetical Markovnikov cyclization.

To address the issue of competing formation of Markovnikov and anti-Markovnikov products during enzyme-catalyzed terpenoid biosynthesis, we have previously used the powerful technique of isotopically sensitive branching.[31] (−)-Pinene synthase is a monoterpene synthase which converts geranyl diphosphate to a mixture of several monoterpenes, including (−)-α-pinene, (−)-*β*-pinene, and (−)-camphene.[32] Cyclization of a deuterated sample of GPP resulted in an increase in the ratio of α-pinene to *β*-pinene, due to the isotope effect on removal of deuterium from the methyl group of the common bicyclic intermediate pinanyl cation **17**, without perturbing the ratio of total α- and *β*-pinenes to camphene[31] (Figure 4B). These results established that the commitment to formation of camphene must take place *before* the isotopically sensitive step and that cyclization of the α-terpinyl cation **18** therefore involves *competing* Markovnikov and anti-Markovnikov cyclizations. Had only Markovnikov cyclization of the α-terpinyl cation been allowed, camphene would have had to be formed by rearrangement of the common pinanyl cation intermediate **17** to the bornyl cation **19** (Figure 4B, pathway c), rather than by direct formation of **19** from the α-terpinyl cation (Figure 4B, pathway b). In such a case, the deuterium isotope effect would have increased the proportion of *both* camphene and α-pinene relative to *β*-pinene. To our knowledge, the isotopically sensitive branching experiment is by far the clearest and least ambiguous demonstration that there is no intrinsic prohibition against enzyme-catalyzed anti-Markovnikov reactions. Such "disfavored" electrophilic additions are presumably facilitated by specific enzymic stabilization of the nominally less stable transition state leading to the secondary carbocationic intermediate. In the pentalenene synthase-catalyzed cyclization of FPP, formation of the secondary humulyl cation **3** is therefore expected to take place directly, without intervention of the otherwise more stable germacradienyl cation **13** (Scheme 5). Formation of (+)-germacrene A (**7**) by the various pentalenene synthase mutants is thus a true *derailment* or diversion of the normal cyclization reaction, and not simply the consequence of trapping of a normally cryptic, cationic intermediate.

Experimental Section

Materials. Sources of reagents and chromatographic materials were as previously described.[6] Expression, purification, and assay of recombinant pentalenene synthase from *E. coli* BL21(DE3)/pZW05 was perfomed as described.[6] Authentic *β*-caryophyllene was obtained from Sigma. Mutagenic oligonucleotides and primers were purchased from IDT. The Altered Sites II in vitro Mutagenesis System and competent cells of ES1301*mut*S and JM109 were obtained from Promega, while *E. coli* BL21(DE3) was purchased from Stratagene. *Eco*RI, *Hin*dIII, and T4 DNA ligase were purchased from Stratagene, and *Age*I, *Ppu*MI, *Sac*I, and *Eco*NI were from New England Biolabs. Plasmid DNA purification was performed using the QIAprep spin Miniprep kit (Qiagen).

General Methods. Restriction endonuclease digestions, DNA ligations, transformation of competent cells, plasmid minipreps, mutagenesis, and other standard recombinant DNA manipulations were carried out by standard methods and according to the suppliers' protocols. dsDNA sequencing was performed by the HHMI Biopolymer/Keck Foundation Biotechnology Resource Laboratory at the Yale University School of Medicine, New Haven, CT, using the dideoxy dye terminator method and automated fluorescence sequencing. Analysis of DNA and protein sequences as well as PCR primer design utilized the suite of programs in the Wisconsin sequence analysis package, version 10.0 (Unix), Genetics Computer Group (GCG), Madison, WI.

Pentalenene Synthase Mutants. The *Eco*RI−*Hin*dIII fragment of pZW05 which harbors the wild-type pentalenene synthase gene[6] was ligated into the Promega vector pALTER-1, and mutations were introduced using the Altered Sites II in vitro Mutagenesis system in combination with the mutagenic primers listed in Table S1 of the Supporting Information. Mutant plasmids were initially screened by restriction digestion to verify the loss or introduction of any relevant restriction sites (Table S1, Supporting Information). The identities of each of the mutations were then directly verified by sequencing of the full-length gene. Each of the mutant genes was then excised by *Eco*RI−*Hin*dIII digestion, ligated back into the T7-based expression plasmid pLM1, and subcloned in *E. coli* XL1 Blue. The resultant mutant plasmids were then used to transform the expression host *E. coli* BL21-(DE3).

Protein Overexpression and Kinetic Studies. Individual strains of *E. coli* BL21(DE3) harboring the mutant plasmids pGZ11 (H309A),

(31) Croteau, R. B.; Wheeler, C. J.; Cane, D. E.; Ebert, R.; Ha, H.-J. *Biochemistry* **1987**, *26*, 5383−5389.
(32) Gambliel, H.; Croteau, R. *J. Biol. Chem.* **1984**, *259*, 740−748.

pGZ12 (H309S), pGZ13 (H309C), pMS11 (H309F), pMS04 (W308F), pMS03 (W308F/H309F), pMS05 (D80E), pMS06 (D81E), pMS08 (D84E), pGZ14 (N219A), pGZ17 (N219L), pMS07 (N219D), and pMS09 (F77Y) were each grown overnight in 50 mL of LB media containing 100 μg/mL ampicillin at 37 °C and 250 rpm. This culture (10 mL) was used to inoculate 500 mL of the same media which was grown for 3 h until $OD_{600} > 0.8$. The culture was transferred to a bath at 30 °C, and after 30 min enzyme production was induced using 0.5 mM IPTG for 3 h. After centrifugation (6000*g*, 25 min), 2.8 g of cells was typically obtained. Lysis of the cells, DNAse treatment, and sonication were performed as for wild-type pentalenene synthase.[6] After PEG precipitation of the undesired proteins and centrifugation (9500*g*, 20 min), the mutant pentalenene synthase was purified as previously described.[6] Kinetic assays were performed as previously described for wild-type pentalenene synthase, except that different ranges of concentration for [1-^{3}H]FPP were used to compensate for the variations in K_m. Steady-state kinetic parameters were determined by direct fitting of the data to the Michaelis−Menten equation by nonlinear least-squares regression using the commercial Kaleidagraph software package.

Mutant Product Analysis. In a typical incubation reaction, 100 μg of purified enzyme was incubated with FPP (50 μM) in a total volume of 1 mL supplemented with kinetics buffer (50 mM Tris-HCl, 5 mM $MgCl_2$, 1 mM DTT, 0.2 mM PMSF, 0.2 mM benzamidine, 20% (v/v) glycerol, pH 8.2) at 30 °C for 1 h, and the aqueous layer was overlaid with 2 mL of HPLC grade pentane. The hydrocarbon products were extracted twice with 1 mL of pentane. The organic layer was concentrated to about 100 μL under reduced pressure at 0 °C. The concentrate was analyzed by GC−MS using a HP-5988A GC−MS system containing a HP-1 column and running the following heating program: 55 °C for 4 min and then 5 °C/min until 210 °C with an injector temperature of 150 °C. Under those conditions, pentalenene (**2**), (+)-germacrene A (**7**), protoilludene (**8**), and β-caryophyllene (**9**) eluted at 15.53, 19.33, 16.45, and 17.30 min, respectively.

Determination of the Stereochemistry of Germacrene A. The germacrene samples from the H309F, H309S, H309C, W308F, and W308F/H309F mutants were each shown to correspond to (+)-germacrene A (**7**). The absolute configuration of (+)-germacrene A was demonstrated by means of its Cope rearrangement to (−)-β-elemene (**9**).[17] The sample in hexane (2 μL) was analyzed by GC−MS (25 m × 0.25 mm i.d. heptakis(6-*O*-TBDMS-2,3-di-*O*-methyl)-β-cyclodextrin (50% in OV17)) using an injection port temperature of 250 °C to induce the rearrangement of enzymatically produced (+)-germacrene A (**7**), with an oven temperature program of 4 min at 45 °C followed by a ramp of 2 °C min^{-1} to 170 °C. Spectra were recorded in the selected ion monitoring mode (*m*/*z* 121, 147, and 189). A racemic β-elemene standard was isolated from the hydrodistillate of the liverwort *Frullania macrocephalum*, and the elution order of its enantiomers was determined with a (−)-β-elemene standard.[18] Under these conditions, (+)-β-elemene and (−)-β-elemene eluted at 31.82 and 31.97 min, respectively.

Crystallography. Purified N219L pentalenene synthase was concentrated to 2−7 mg/mL using Centricon filter devices (Amicon) and used in sitting-drop batch crystallization trials at room temperature: various protein concentrations [2.0, 4.5, and 6.6 mg/mL N219L pentalenene synthase in 100 mM HEPES (pH = 7.0)], protein solution volumes, and precipitant buffer volumes were sampled in 3 × 3 Pyrex (Corning) grids sealed in plastic containers and equilibrated against 35 mL of precipitant buffer [1.5 M ammonium sulfate, 100 mM Tris-HCl (pH = 8.2)]. The optimal composition of sitting drops was 40 μL of enzyme solution and 20 μL of precipitant buffer, which yielded hexagonal, rodlike crystals of approximate dimensions 0.2 mm × 0.2 mm × 0.4 mm within 3 weeks. These crystals were prepared for X-ray data collection by gradual transfer into a 30% glycerol cryoprotectant solution and flash-cooled in liquid propane for transport to the Stanford Synchrotron Radiation Laboratory (Beamline 7-1). X-ray diffraction data were collected using a MAR 345/CCD image plate system (300 mm plate, crystal-to-detector distance = 120 mm, λ = 1.08 Å). Crystals of N219L pentalenene synthase were isomorphous with those of the wild-type enzyme.[8a] A total of 63 768 measured reflections yielded 23 110 unique reflections, 97% complete to 2.9 Å resolution (R_{sym} = 0.083). Data integration and reduction was performed using the HKL program suite,[33] and corrected structure factor amplitudes were generated with routines contained in the CCP4 program suite.[34]

Initial phases for the electron density map of N219L pentalenene synthase were obtained by molecular replacement against 20−4 Å data using routines contained in CNS[35] and residues 9−304 of the wild-type pentalenene synthase crystallization dimer as a search probe.[8a] The cross-rotation function and subsequent translation searches yielded an unambiguous solution with a correlation coefficient significantly higher than those for all other solutions (0.436 with the next closest peak at 0.197): $\alpha = 114.69°$, $\beta = 175.81°$, $\gamma = 52.28°$, $x = 0.83$, $y = -3.60$, $z = -1.88$. Rigid-body refinement lowered the initial *R* factor from 0.455 to 0.432, and subsequent refinement employed torsion angle dynamics with energy minimization ($T_{initial}$ = 5000 K), using the maximum likelihood algorithm implemented in CNS.[35] Model building was performed using O.[36] Strict noncrystallographic symmetry constraints and grouped *B* factors (one main chain and one side chain per residue) were initially imposed in refinement. However, improved convergence was achieved when a bulk solvent correction was applied, when restrained individual *B* factors were utilized, and when noncrystallographic symmetry constraints were converted to highly weighted restraints (w = 100−300 kcal mol^{-1}) in loop regions. Residues 7−311 were fit into the final electron density map along with a total of 26 water molecules.

Refinement converged smoothly to a final crystallographic *R* factor of 0.263 (R_{free} = 0.308). The final model had excellent stereochemistry: root-mean-square (rms) deviations from ideal bond lengths and angles were 0.009 Å and 1.3°, respectively, and analysis with PROCHECK[37] indicated 464, 48, and 2 nonproline/nonglycine residues in both molecules of the asymmetric unit with most favored, additionally allowed, and generously allowed backbone conformations, respectively. Refined atomic coordinates of N219L pentalenene synthase have been deposited in the Research Collaboratory for Structural Bioinformatics with PDB accession code 1HM7.

Acknowledgment. This research was supported by an NIH Merit Award (GM30301) to D.E.C. and an NIH Grant (GM56838) to D.W.C. We also thank F. Verstappen for technical assistance and Prof. W. A. König of Hamburg University, Germany, for the gift of the β-elemene standards.

Supporting Information Available: Table S1 listing mutagenic primers for generation of pentalenene synthase mutants, and GC−MS chromatograms from analysis of enzymatic formation of (+)-germacrene (**7**) (PDF). This material is available free of charge via the Internet at http://pubs.acs.org.

JA026058Q

(33) Otwinowski, Z.; Minor, W. *Methods Enzymol.* **1997**, *276*, 307−326.
(34) Collaborative Computational Project, Number 4. *Acta Crystallogr.* **1994**, *D50*, 760−763.
(35) Brünger, A. T.; Adams, P. D.; Clore, G. M.; Gros, P.; Grosse-Kunstleve, R. W.; Jiang, J. S.; Kuszewski, J.; Nilges, N.; Pannu, N. S.; Read, R. J.; Rice, L. M.; Simonson, T.; Warren, G. L. *Acta Crystallogr.* **1998**, *D54*, 905−921.
(36) Jones, T. A.; Zou, J.-Y.; Cowan, S. W.; Kjeldgaard, M. *Acta Crystallogr.* **1991**, *A47*, 110−119.
(37) Laskowski, R. A.; MacArthur, M. W.; Moss, D. S.; Thornton, J. M. *J. Appl. Crystallogr.* **1993**, *26*, 283−291.
(38) Swiss-Pdb Viewer (Deep View): http://www.expasy.ch/spdbv/mainpage.htm
(39) Nicholls, A.; Honig, B. *J. Comput. Chem.* **1991**, *12*, 435−445.
(40) Kraulis, P. J. *Appl. Crystallogr.* **1991**, *24*, 946−950.
(41) Bacon, D. J.; Anderson, W. F. *J. Mol. Graph.* **1988**, *6*, 219−220. Merritt, E. A.; Murphy, M. E. P. *Acta Crystallogr.* **1994**, *D50*, 869−873.